the strongest texture components are cube and various forms of cube rotated around the normal of the rolling plane. Typical rolling texture components are found in the depths closer to mid thickness. At 3T/8, copper, brass and S are present in all plates, cube texture at a lower level is also found. At mid thickness brass becomes dominant in all the three plates. The dominance of brass is larger for the 100 and the 200mm plate compared to the 150mm plate. The strongest texture is found in the 200mm plate. This suggests that the yield strength anisotropy is pronounced in the 200mm plate. This seems true for the through thickness variation, but not for the planar anisotropy, see Fig. 3c). The grain morphology differs between the plates. The 100 and 150mm plates show similarities. The grains are flat and elongated, their mean sizes are smaller close to the surface. Grain size in the intermediate layers are slightly larger compared to the size at the centre depth [11]. It is also shown in the same reference that the size of the grains in the more reduced plate are slightly smaller compared to the grains in the 150mm plate. However the grain morphology of the 200mm plate is different from the less thick plates. Here the grains are extremely pancake shaped, as could be seen in Fig. 2a). For sheet material this elongated, unrecrystallised grain structure is known to be beneficial for fracture toughness properties [6].

4. Conclusions

- Micro hardness of recrystallised grains compared to recovered grains did not show any significant differences. Properties of flow stress was not significantly affected by subgrain boundaries.
- Recrystallisation did not show any detrimental effect on fracture toughness.
- EBSP mappings showed that recrystallisation not only took place through PSN, but also probably through subgrain growth at grainboundaries within PFZs with sequential SIBM.

Acknowledgement

The authors would like to thank Hoogovens Aluminium Walzprodukte GmbH for the supply of material and test results used in this investigation, Dimitris Apatsidis, Håkan Brodin and Dr Bernt Jaensson for his advice in planning this work.

References

1. Reynolds, M.A., P.E. Fitzsimmons, and J.G. Harris. . 1976. Turin, Italy.
2. Chakrabarti, D.J., *et al.*, Materials Science Forum, 1996. **217-222**: p. 1085-1090.
3. Ehrström, J.C., *et al.* in *The 4th international conference on aluminium alloys*. 1994. Atlanta, Georgia, USA.
4. Brown, K.R. in *ICSMA 6*. 1982. Melbourne: Oxford Pergamon.
5. Dorward, R.C. and D.J. Beerntsen, Metallurgical and Materials Transactions A, 1995. **26A**(September): p. 2481-2484.
6. Thompson, D.S., Metallurgical Transactions A, 1975. **6A**(April): p. 671-683.
7. Lapasset, G. and C. Renon, La Recherche Ae´rospatiale, 1982. **5**(September-October): p. 313-326.
8. Apatsidis, D., . 1997, Institute of Technology, Dept of Mech Eng: Linköping. Rep. nr.:LiTH-IKP-Ex-1433
9. Andersson, N.E., X.H. Zeng, and S. Johansson. in *Thermo- Mechanical Processing Theory, Modelling and Practice (TMPT)2*. 1996. Stockholm.
10. Engler, O., *et al.*, Materials Science and Technology, 1996. **12**(September): p. 717-729.
11. Johansson, S., N.-E. Andersson, and X.-H. Zeng. in *THERMEC'97*. 1997. University of Wollongong, Australia: TMS.
12. Humphreys, F.J. and M. Hatherly, *Recrystallisation and related annealing phenomena*. 2 ed. 1996: Pergamon. 497.
13. Ehrström, J.C., *et al.* in *ICAA4*. 1994. Atlanta USA.
14. Brodin, H., . 1997, Institute of Technology, Linköping. Rep. nr:LiTH-IKP-S-453

THERMAL-MECHANICAL PROCESSING OF ELECTRICAL CONDUCTOR GRADE ALUMINUM TO INDUCE CONTINUOUS RECRYSTALLIZATION

Haiou Jin*, Jian Li** and S. Saimoto*

* Department of Metallurgical and Materials Engineering, Queen's University, Kingston, Ontario, Canada K7L 3N6

** Fibics Inc., 568 Booth Street, Ottawa, Ontario, Canada K1A 0G1

ABSTRACT A well homogenized electrical conductor grade Al was intermediately annealed at 230 °C after 21% reduction to getter the Fe solutes. Subsequent cold rolling 86.7% to 4mm and recrystallization at 320 °C resulted in a mean grain size of 40 μm. The 0.76mm rolled sheet upon recrystallization at 220 °C, 275 °C and 320 °C manifested continuous recrystallization with slow rate of grain growth during which period the hardness gradually decreased. This decrease in hardness was attributed to dipole and/or loop annihilation. Upon the inception of secondary recrystallization the cube texture became very prominent.

Keywords: *Aluminum, continuous recrystallization, fine grain size, texture*

1. INTRODUCTION

The continuing interest in ultra-fine grain size refinement has again revealed a phenomenon described as continuous recrystallization(CREX)[1]. Our recent studies in nominally pure aluminum indicate that a distinct morphological change between discontinuous recrystallization and a finely equiaxed structure occurs when the solute Fe impurity level becomes less than 1 atomic ppm[2,3]. Moreover if the impurity level reaches below 0.01 ppm, dynamic recrystallization appears to take place even at room temperature[4]. Electron back scattered diffraction patterns reveal that indeed the grain boundary mis-orientations across these micrometer scale grains are large angles. Furthermore, Furu and Nes[5] had shown that in a slow cooled Al-Fe alloy the discontinuous grain growth(DGG) of the largest grains when extrapolated to zero time results in intercepts at values less than 10 μm. The nature of this fine structure can be examined more carefully by electron channeling contrast(ECC) in the scanning electron microscope(SEM) whereby the substructure due to deformation and sub-structure free equiaxed grains can be differentiated. In the present study, electrical conductor grade(EC) Al was used to further delineate the conditions required to produce CREX and wherein the process textural evolution occurs.

2. DESIGN OF EXPERIMENT

After homogenization of an Al-Fe ingot, the grain size is usually very large due to the very low solubility of Fe in Al. On the other hand for deformation texture and recrystallization studies, finer grain sizes of the order of 50 μm are most desirable. To obtain this desired microstructure with a very low matrix Fe content, the alloy has to be equilibrated at a low temperature for a long time dictated by $\sqrt{Dt}$ where D is the diffusivity of Fe in Al and t, the holding time at a certain temperature. To accelerate this process, prestraining was used to introduce dislocations which can act as heterogeneous sites for precipitation[6]. Extrapolation of an accurate Al-Fe solvus[7] indicates that the solubility of Fe is 14 ppb at 230 °C, 74 ppb at 275 °C, and 310 ppb at 320 °C. As a starting base our typical procedure is to hold for 100 hr at 230 °C after 20% reduction in area. Subsequent to this anneal the material is cold worked and its recovery, recrystallization and grain growth are systematically studied using hardness testing, ECC-SEM, orientation distribution function(ODF) from X-ray pole figures and qualitative peak broadening[8].

3. EXPERIMENTAL PROCEDURES

A block, 60mm long, 50mm wide and 38mm thick, was cut from a disc of as-cast EC grade Al ingot and then homogenized for 24 hours at 600 °C. The composition of the ingot in atomic ppm is 2060Fe-306Cu-165Ga-90B-39V-31Zn. The grains were oblong about 1mm^2 in cross section and a few mm long. The rolling surface was set perpendicular to the long length. After cold rolling to 30 mm thickness and annealing at 230 °C for 100 hours, the block was further cold rolled 86.7% down to a thickness of 4 mm. Small pieces from the 4mm slab were annealed at 230 °C, 275 °C, 300°C and 320 °C for 1 to 2 hours. After 2 hours at 320 °C the sample fully recrystallized with a uniform grain size of about 40μm. Hence the 4mm thick slab was annealed at 320 °C for 2 hours and subsequently cold rolled to the final thickness of 0.76 mm. All rolling was carried out without reversal of ends or surfaces. Small samples of 22mm×14mm were cut from the 0.76 mm sheet and heat treated at 220 °C for 180s to 10h, at 275 °C for 10 to 600s and at 320 °C for 3 to 120s, respectively. The electropolished surfaces parallel to the rolling surface were examined by ECC in a JSM-840 SEM. The grain size was determined from ECC-SEM micrographs of 2200 times magnification using the Heyn intercept method, and the texture evolution was measured using ODF analysis of van Houtte[9]. Pole figures were measured at various depths from the sample surface, i.e., 0.05 mm, 1/4 thickness and 1/2 thickness(central layer). ODF analysis was done using monoclinic rather than orthorhombic sample symmetry due to the asymmetry of the measured pole figures[10]. Micro-hardness using 25g load(Vickers), residual line broadening of (311) peaks, and grain size were measured at the central layer of samples. Following the method of Hu[8] a Rigaku Model RINT 1100L line focus diffractometer equipped with a graphite monochromator was used to determine an arbitrary parameter $B = (I_{min}-I_b)/(I_{max}-I_b)$ where I_{min} is the intensity minimum between $K\alpha_1$ and $K\alpha_2$ peaks of the Cu $K\alpha$ radiation, I_{max} is the intensity of the $K\alpha_1$ peak and I_b is the background intensity. The term fraction residual line broadening, F_B, refers to $(B_T-B_{REX})/(B_{CR}-B_{REX})$ where the subscripts T refers to the condition after different times of annealing at temperature T, REX to the completely recrystallized state and CR to the cold rolled one.

4. RESULTS

4.1. Texture Evolution

After the intermediate anneal at 230 °C, the estimated Fe solute level is 14 ppb. The subsequent cold rolling of 30mm to 4mm resulted in a nearly monoclinic pole figure about the X_1 axis as shown in Fig. 1a, which upon recrystallization at 320 °C became triclinic (Fig. 1b). The reason for this unexpected result must be due to the large starting grain size and the high purity of the matrix. During the anneal at 320 °C for 2h, some of the Al-Fe intermetallic precipitates would have dissolved to equilibrate the Fe content of the matrix at 310 ppb. Upon cold rolling the recrystallized slab, a texture which is still monoclinic but reminiscent of the typical rolled texture for nominally pure aluminum was found(Fig. 1c). During subsequent annealing and the occurrence of primary recrystallization, this texture pattern did not change(Fig. 1d) until the secondary recrystallization took place, whereby the cube texture component coexisted with the rolling texture. Such observation has been previously reported[11].

4.2. Microstructural Evolution and Fraction Residual Line Broadening

Figure 2a shows an ECC micrograph illustrating a mixed structure of continuously recrystallized and deformed structure after recovery. The CREX grain size can be determined, but in the unrecrystallized ribbon-like structure the sub-grain boundaries are not clearly resolvable. The initiation of DGG is shown in Fig. 2b whereby an occasional large abnormal grain has appeared and the proportion of these large grains increases with increase in temperature. Fig. 3a shows the measured grain sizes for both the CREX grains and the largest ones observed. The normal grain

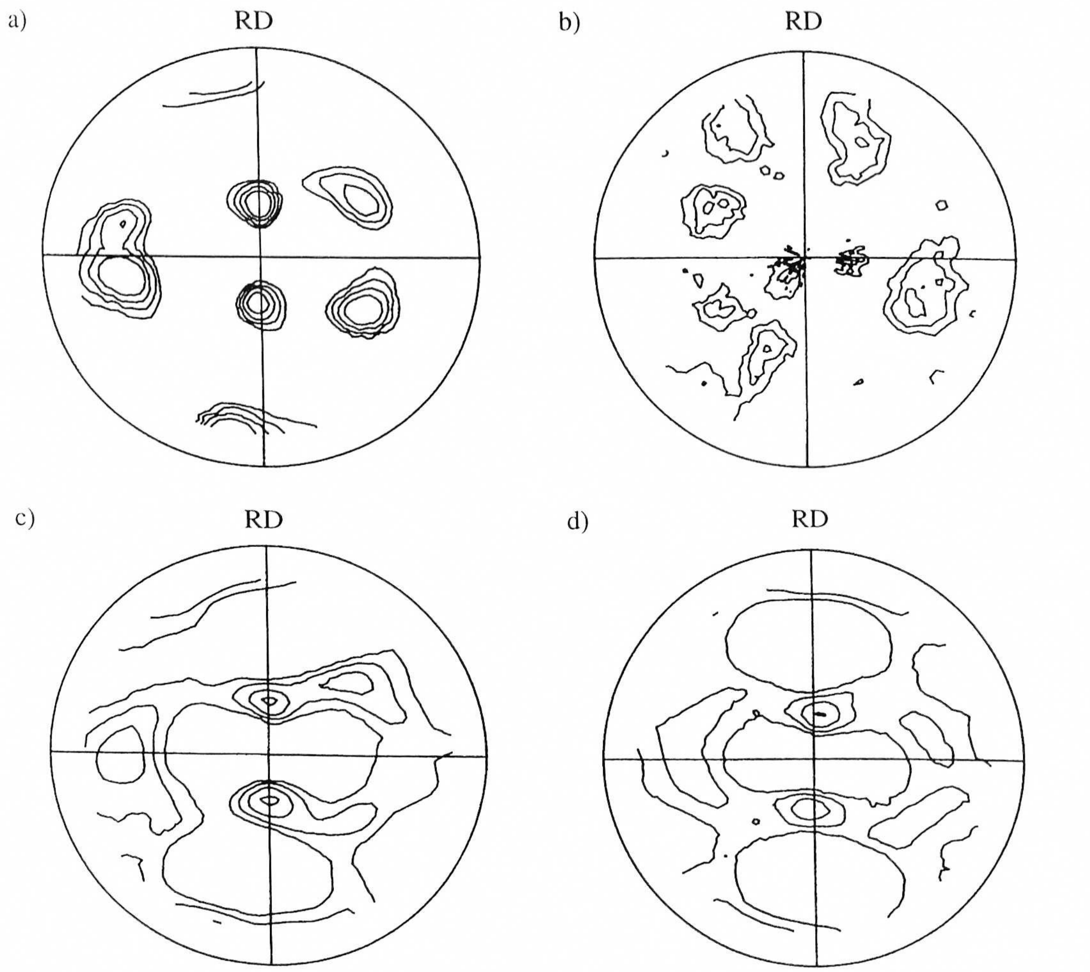

Fig. 1. The (111) pole figures of a) 4mm thick sample as-rolled, b) 4mm thick sample annealed at 320 °C for 2h, c) 0.76mm thick sample as-rolled and d) 0.76mm thick sample annealed at 220 °C for 2h. The contour levels are 1, 2, 4, 8 times random.

growth relation (D^n-D_0^n = kt) was difficult to evaluate for the fine grains. A rough estimate is that n is near 1/5 which suggests that grain boundary migration is controlled by precipitate coarsening along dislocation lines. The area fraction of the large grains is difficult to measure but ODF analysis shows that upon the appearance of DGG the cube texture volume fraction increases(Fig. 3b). The micro-hardness result shown in Fig. 4 suggests that there is a break of the continuous hardness decrease at the time the metallographic evidence shows the inception of DGG. However F_B shows a more or less unchanging value in this interval after a dramatic drop upon CREX. As DGG progresses this parameter asymptotically approaches zero.

5. DISCUSSION

The ODF evidence suggests that the global texture for CREX is similar to the as-deformed one while the micro-texture between the fine grains can be large. In the present study, although F_B shows a sharp drop corresponding to the metallographic observation of structure change, the micro-

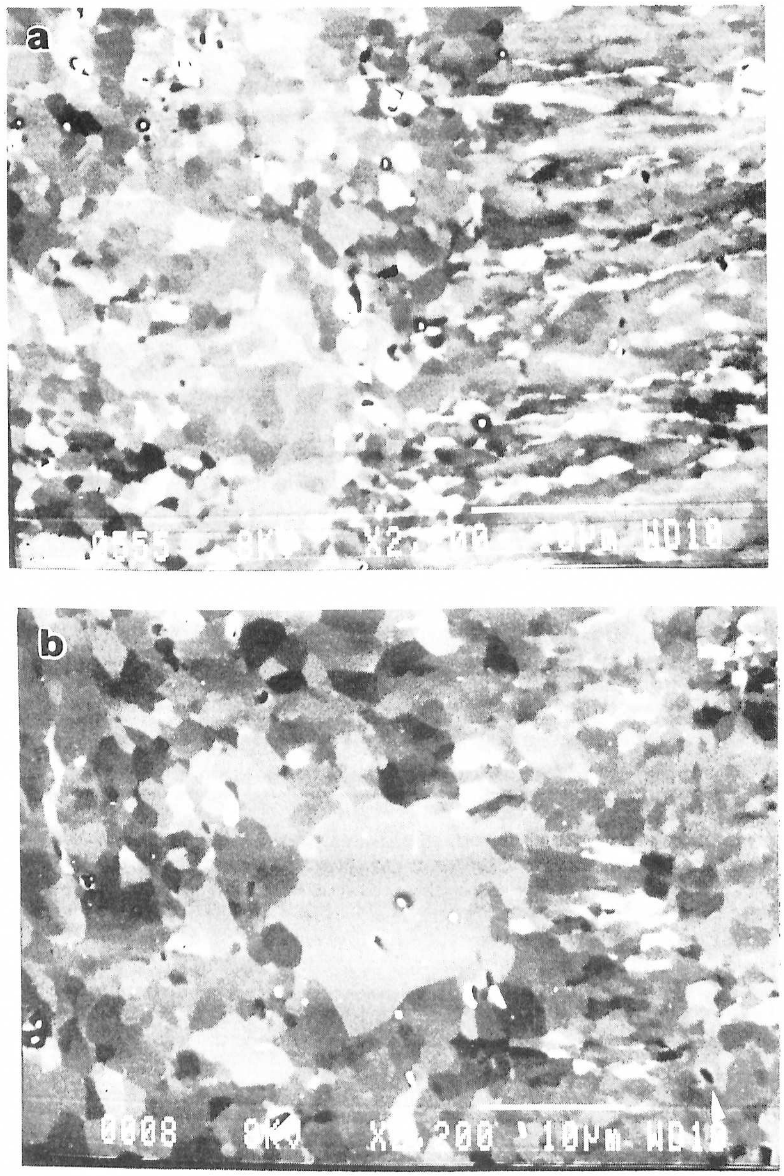

Fig. 2. ECC-SEM micrographs of a) the mixed structure of very fine grains of CREX(left half) and recovered structure(right half) in the 0.76mm sample annealed at 320 °C for 3 sec, and b) an example of sparse large grains among CREX grains in the 0.76mm sample annealed at 275 °C for 37 sec.

hardness as a function of time at temperature only manifests a gradual change. However a hardness plateau, H_0, at about HV 40 is apparent prior to DGG. Thus if a change in hardness $\Delta H = H - H_0$ is defined as recovery due to dipole strengthening[12], it can be plotted as $1/\Delta H^2$ versus time and an activation energy corresponding to Q = 1.57 eV is found. Using this value the isothermal hardness values at various temperature can be collapsed into a common curve using compensated temperature time(Fig. 5). Furthermore, a bifurcation is observed upon the inception of DGG indicating a pre-emptive change in mechanisms. This analysis suggests that the hardness decrease is due to the annihilation of dipoles which will not contribute to peak broadening. Moreover, the initial drop in peak broadening does not affect the flow stress since in the Mughrabi composite work hardening analysis[13] the internal stress does not explicitly affect the applied flow stress due to intrinsic cancellation. Thus a self-consistent rationale for the present observations is at hand. The issue of the initiation of DGG is attributed to the role of Fe solutes keeping in mind that increasing the temperature not only increases the thermal energy for grain boundary migration but also increases the Fe solubility. The increased Fe solute begins to affect the migration of random grain boundaries with the least effect on specific low energy type such as the $\Sigma 7$, which is formed between the cube and S texture components. Detailed discussion of this analysis will appear elsewhere[2].

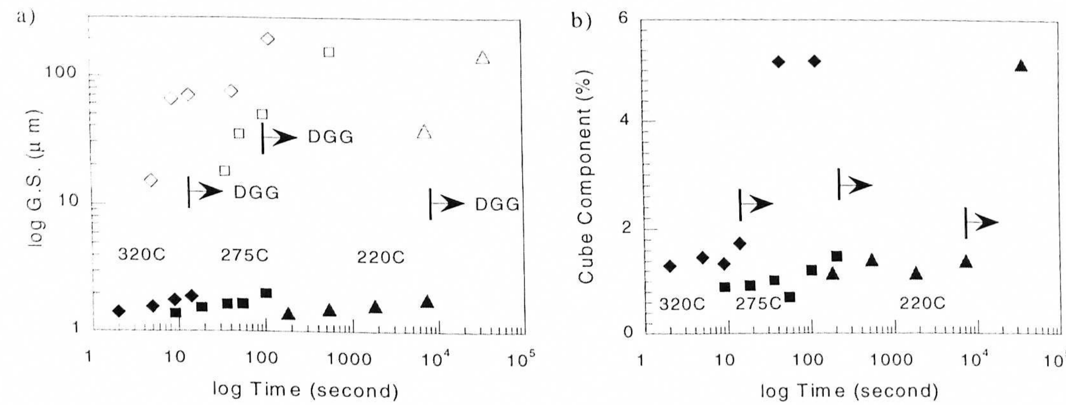

Fig. 3. Time dependence of a) Grain size of CREX(filled symbols) and the largest grain observed(open symbols) in 0.76mm annealed samples. b) Volume fraction of cube texture component. The marked inception of DGG infers that the volume fraction of large grains exceeds 5%.

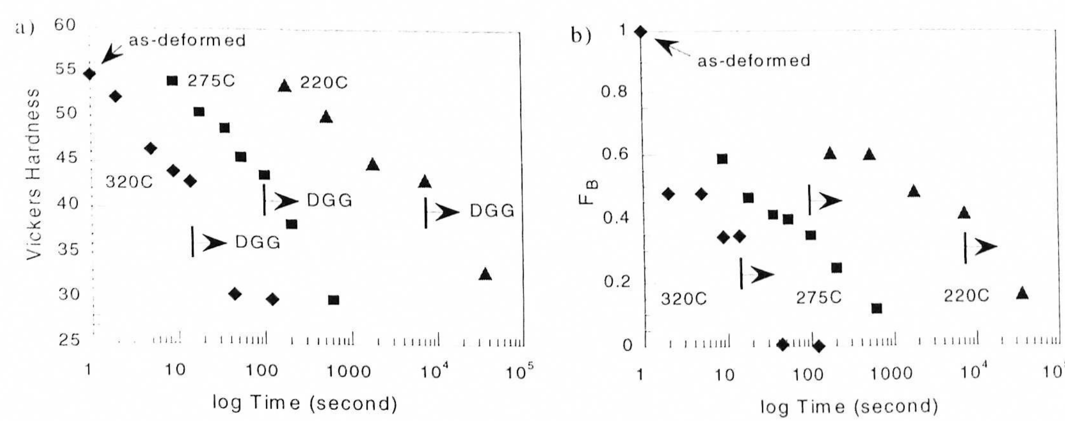

Fig. 4. Vickers hardness versus log time showing the three isothermal curves with an abrupt break near $H_0 = 40$. b) Fraction residual line broadening corresponding to the hardness curves. Note the abrupt initial drop of at least 40%.

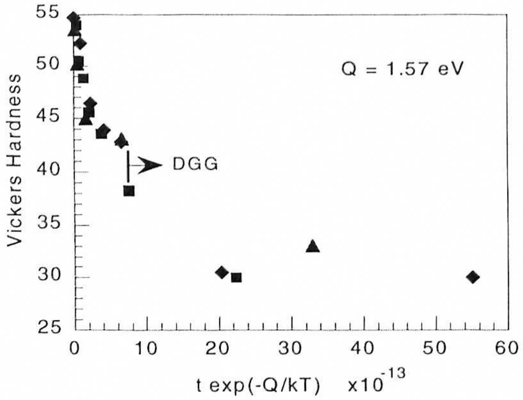

Fig. 5. Temperature compensated time curve of the hardness values collapsing the data into a common line prior to the bifurcation after the inception of DGG.

ACKNOWLEDGEMENTS

The authors gratefully acknowledge the support of Ontario Centre for Materials Research and the Natural Science and Engineering Research Council of Canada. We thank Alcan International Ltd. for especially preparing the EC grade aluminum in a form suitable for rolling and/or hot extrusion.

REFERENCES

[1] Jian Li and S. Saimoto, Materials Sci. and Eng. **A 234-236** (1997), 1011.
[2] Jian Li and S. Saimoto, Materials Science Forum, (1998), in press.
[3] S. Saimoto, Jian Li, G. Langelaan, B. Diak and J. Shimizu, Textures and Microstructures, **26-27** (1996), 245.
[4] Jian Li, Ph.D. Thesis, Queen's University at Kingston, Canada, (1997).
[5] T. Furu and E. Nes, Materials Science Forum, **113-115** (1993), 311.
[6] H. Legace and S. Saimoto, in Annealing Process-Recovery, Recrystallization and Grain Growth, ed. H. Hansen *et.al*, Riso, Denmark, (1986), 415.
[7] B. J. Diak, Ph.D. Thesis, Queen's University at Kingston, Canada, (1997).
[8] Hsun Hu and S. R. Goodman, Metallurgical Transactions, **1** (1970), 3057.
[9] P. van Houtte, Textures and Microstructures, **6** (1984), 137.
[10] S. Saimoto, R. G. Kamat, P. Clark and P. van Houtte, Textures and Microstructures, **21** (1993), 109.
[11] J. Grewen and M. Heimendahl, Zeit. Metallkunde, **59** (1968), 205.
[12] G. van Drunen and S. Saimoto, Acta Metall. **19** (1971), 213.
[13] F. R. N. Nabarro, Acta Metall. **37** (1989), 1521.